

# A systematic study on the reactivity of different grades of charged $\text{Li}[\text{Ni}_x\text{Mn}_y\text{Co}_z]\text{O}_2$ with electrolyte at elevated temperatures using accelerating rate calorimetry

Lin Ma <sup>a</sup>, Mengyun Nie <sup>b</sup>, Jian Xia <sup>b</sup>, J.R. Dahn <sup>a, b, \*</sup>

<sup>a</sup> Department of Chemistry, Dalhousie University, Halifax, B3H 4R2, Canada

<sup>b</sup> Department of Physics and Atmospheric Science, Dalhousie University, Halifax, B3H 3J5, Canada

---

## H I G H L I G H T S

- $\text{Li}[\text{Ni}_{0.8}\text{Mn}_{0.1}\text{Co}_{0.1}]\text{O}_2$  shows serious reactivity with electrolyte above 110 °C.
- $\text{Li}[\text{Ni}_{0.4}\text{Mn}_{0.4}\text{Co}_{0.2}]\text{O}_2$  shows the least reactivity with electrolyte at high temperature.
- $\text{Li}[\text{Ni}_{0.6}\text{Mn}_{0.2}\text{Co}_{0.2}]\text{O}_2$  and  $\text{Li}[\text{Ni}_{0.5}\text{Mn}_{0.3}\text{Co}_{0.2}]\text{O}_2$  show intermediate reactivity.
- This work identifies important trade-offs between  $\text{Li}[\text{Ni}_x\text{Mn}_y\text{Co}_z]\text{O}_2$  grades.

---

## A R T I C L E I N F O

### Article history:

Received 11 February 2016

Received in revised form

24 May 2016

Accepted 11 July 2016

Available online 22 July 2016

### Keywords:

Lithium ion cells

Different NMC grades

Systematic comparison

Safety

Accelerating rate calorimetry

---

## A B S T R A C T

The reactivity between charged  $\text{Li}[\text{Ni}_x\text{Mn}_y\text{Co}_z]\text{O}_2$  (NMC, with  $x + y + z = 1$ ,  $x:y:z = 1:1:1$  (NMC111), 4:4:2 (NMC442), 5:3:2 (NMC532), 6:2:2 (NMC622) and 8:1:1 (NMC811)) and traditional carbonate-based electrolytes at elevated temperatures was systematically studied using accelerating rate calorimetry (ARC). The ARC results showed that the upper cut-off potential and NMC composition strongly affect the thermal stability of the various NMC grades when traditional carbonate-based electrolyte was used. Although higher cut-off potential and higher Ni content can help increase the energy density of lithium ion cells, these factors generally increase the reactivity between charged NMC and electrolyte at elevated temperatures. It is hoped that this report can be used to help guide the wise selection of NMC grade and upper cut-off potential to achieve high energy density Li-ion cells without seriously compromising cell safety.

© 2016 Elsevier B.V. All rights reserved.

---

## 1. Introduction

Li-ion batteries (LIB) are now widely used in numerous applications, from portable electronics to electrified vehicles. In order to meet the increasing demands of these applications, the development of advanced positive electrode is critical to help increase the energy density and safety of LIB [1].

The most common positive electrode material is layered structured lithium cobalt oxide,  $\text{LiCoO}_2$

showed that NMC111 had the best safety properties when compared to LCO and NCA. Since nickel-rich NMC can deliver high specific capacity, which contributes to high energy density, Li<sub>0.5</sub>Mn<sub>0.3</sub>Co<sub>0.2</sub>O<sub>2</sub> (NMC532) [14], Li<sub>0.6</sub>Mn<sub>0.2</sub>Co<sub>0.2</sub>O<sub>2</sub> (NMC622) [15] and Li<sub>0.8</sub>Mn<sub>0.1</sub>Co<sub>0.1</sub>O<sub>2</sub> (NMC811) [16,17] have drawn lots of attention as well. A recent excellent review by Kim et al. [10], compares the various tradeoffs between these common NMC grades and shows that the reactivity of these materials with electrolyte at elevated temperature increases with Ni content.

An alternative approach to high energy and lower cost NMC materials is to use materials from the Li[Ni<sub>x</sub>Mn<sub>x</sub>Co<sub>1-2x</sub>]O<sub>2</sub> series with high Mn content and charge cells to high potential. For example, Paulsen et al. [18] promoted Li[Li<sub>x</sub>(Ni<sub>0.42</sub>Mn<sub>0.42</sub>Co<sub>0.16</sub>)<sub>1-x</sub>]O<sub>2</sub> with x near 0.11 as an excellent positive electrode material with exceptional thermal stability compared to Ni-rich materials (See drawing 9 in the patent). Such materials have evolved to be called NMC442 and have been extensively studied by our group recently. Unlike NMC111, which appears to be structurally unstable during extended periods at high potential (>4.5 V) [19], NMC442 did not show any structural changes after sequential exposures to 4.7 and 4.9 V [20]. With appropriate electrolyte additives (NMC442)/graphite full cells have been shown to be able to be operated to 4.4 V for extended periods of time and for 500 cycles (>80% capacity retention) [21] and up to 4.5 V for 500 cycles (>80% capacity retention) [22].

Li-ion battery safety is a key factor and is influenced by the selection of the positive electrode material and the operating potential range. For example, how does the reactivity of NMC442 charged to 4.4 V compare to that of NMC811 charged to 4.1 V? There are no literature references that compare the reactivity between all NMC materials, charged to various potentials, and electrolyte at elevated temperatures using accelerating rate calorimetry. In this work, the reactivity of charged NMC111, NMC442, NMC532, NMC622 and NMC811 at different cut-off voltages with electrolyte was systematically investigated and compared using accelerating rate calorimetry (ARC). The data in this paper can be used to rank the thermal stabilities of charged NMC grades in traditional carbonate-based electrolytes. The advantage of some particular NMC materials at high voltage is revealed from a safety perspective.

## 2. Experimental

1.0 M LiPF<sub>6</sub> in ethylene carbonate (EC):ethyl methyl carbonate (EMC) (3:7 by weight, from BASF, water content was 12.1 ppm) was used as the control electrolyte.

### 2.1. Pouch cells

Dry (no electrolyte) NMC111/graphite, NMC442/graphite, NMC532/graphite NMC622/graphite and NMC811/graphite pouch cells balanced for 4.7 V operation were obtained from Li-Fun Technology (Xinma Industry Zone, Golden Dragon Road, Tianyuan District, Zhuzhou City, Hunan Province, PRC, 412000). The positive electrodes were made with a weight ratio of active material, carbon black and polyvinylidene fluoride (PVDF) binder of 96:2:2. Since the reaction rate at elevated temperatures during ARC testing depends on the surface area of electrode materials in contact with

electrolyte [23], Table 1 shows a summary of the BET specific surface areas of all the NMC positive electrode materials. Fig. 1 shows the scanning electron microscope (SEM) images of the different NMC grades. The NMC442 used in these cells was supplied by Umicore (Chonan, Korea) while the other NMC grades were provided by Chinese suppliers.

All pouch cells were vacuum sealed without electrolyte in a dry room in China and then shipped to our laboratory in Canada. Before electrolyte filling, the cells were cut just below the heat seal and dried at 80 °C under vacuum for 12 h to remove any residual water. Then the cells were transferred immediately to an argon-filled glove box for filling and vacuum sealing. All the pouch cells were filled with 0.9 g of electrolyte. After filling, cells were vacuum-sealed with a compact vacuum sealer (MSK-115A, MTI Corp.). First, cells were placed in a temperature box at 40 ± 0.1 °C where they were held at 1.5 V for 24 h, to allow for the completion of wetting. Then, all the cells were charged at the current corresponding to C/20 to 3.5 V. After this step, all the cells were transferred and moved into the glove box, cut open to release any gas generated and then vacuum sealed. Then all the cells were charged at the current corresponding to C/20 to 4.5 V. After this step, all the cells were transferred and moved into the glove box, cut open to release any gas generated and then vacuum sealed again.

### 2.2. Accelerating rate calorimetry (ARC) experiments

After degassing, all the cells were discharged to 2.8 V. Then the cells were divided into four groups. Each group was charged to its selected upper cut-off potential (4.2 V, 4.4 V, 4.5 V or 4.7 V) at C/20. All the cells were then held at the set upper cut-off potential for around 3 h. After this step, the cells were transferred and moved into the glovebox and cut open to recover the jelly rolls. The jelly rolls were then unwound to get the positive electrode. All the charged NMC powder for the ARC tests was obtained by carefully scratching the electrodes. This was very time consuming because the electrodes were well-adhered to the Al foil current collectors.

In order to make the results comparable, the capacity that had been delithiated from each sample used in the ARC tests was kept the same (~15 mAh). This was done by adjusting the mass of charged positive electrode material added to each ARC sample tube. The following example shows how the mass of material to be added to each ARC tube was determined.

The mass of positive electrode material in an NMC111/graphite pouch cell was 1.14 g. When the cell was charged to 4.2 V, the capacity was ~175 mAh. So the specific capacity,  $Q_{\text{specific}}$ , of the NMC111 material charged to 4.2 V was:

$$Q_{\text{specific}} = 175 \text{ mAh} / (1.14 \text{ g} \times 0.96) = 160 \text{ mAh/g}$$

The number of moles, n, of delithiated lithium was:

$$n = 160 \text{ mAh/g} \cdot 3.6 \text{ C/mAh} \cdot M/F = 0.576$$

where M = 96.5 g/mole is the formula weight of NMC111 and F is Faraday's number in C/mole.

Thus the delithiated NMC111 at 4.2 V can be described as Li<sub>(1-0.576)</sub>[Ni<sub>1/3</sub>Mn<sub>1/3</sub>Co<sub>1/3</sub>]O<sub>2</sub>, or Li<sub>0.424</sub>[Ni<sub>1/3</sub>Mn<sub>1/3</sub>Co<sub>1/3</sub>]O<sub>2</sub>. The mass, m, of delithiated material required for the ARC test is therefore:

**Table 1**  
Summary of the specific surface area for the positive electrode materials in the NMC111/graphite, NMC442/graphite, NMC532/graphite, NMC622/graphite and NMC811/graphite pouch cells. The instrumental error in each value is estimated to be ±0.03 m<sup>2</sup>/g.

Material	NMC111	NMC442	NMC532	NMC622	NMC811
Specific surface area (m <sup>2</sup> /g)	0.34	0.38	0.28	0.24	0.25

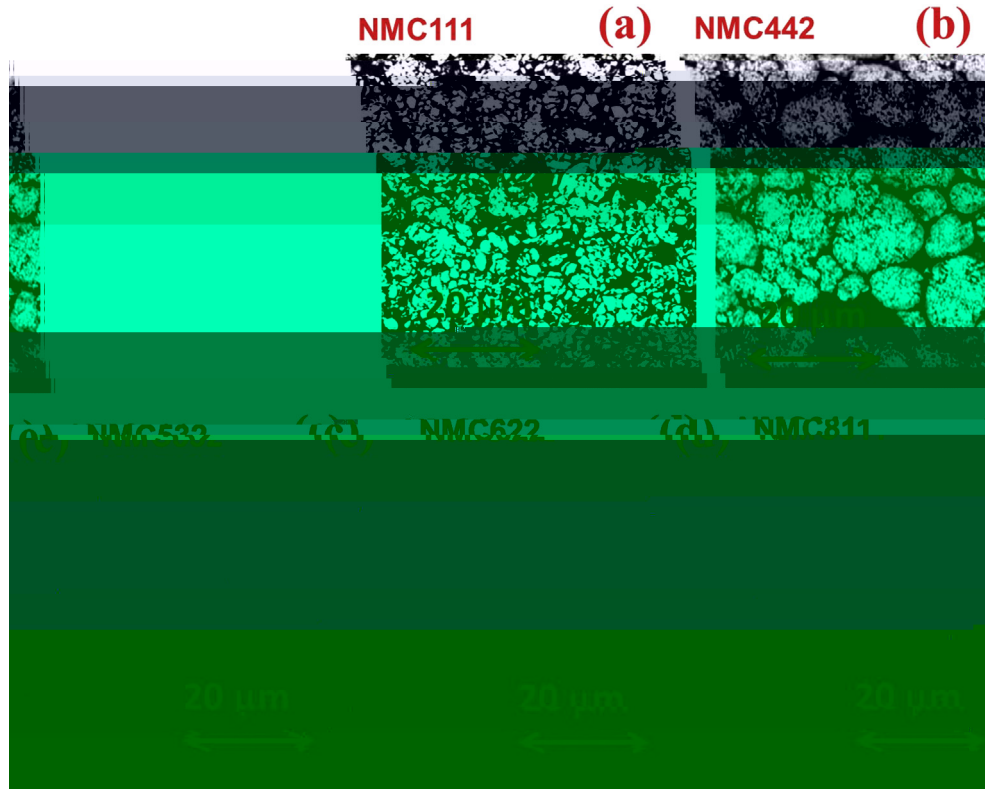


Fig. 1. SEM images of (a) NMC111, (b) NMC442, (c) NMC532, (d) NMC622 and (e) NMC811 used for the ARC tests.

$$m = (15 \text{ mAh}/160 \text{ mAh/g}) \cdot (92.5/\text{M})/0.96$$

In the equation above, 92.5 (g/mole) is the formula weight of  $\text{Li}_{0.424}[\text{Ni}_{1/3}\text{Mn}_{1/3}\text{Co}_{1/3}]\text{O}_2$  and 0.96 is the active mass fraction of the electrode.

Table 2 shows the full cell capacity, specific capacity, delithiated NMC chemical formula and formula weight for the ARC test samples. The electrode:electrolyte mass ratios were also kept the same for all the tests. Table 3 lists the amount of electrode material and electrolyte used for the ARC tests. The ARC starting temperature

was set at 70 °C. ARC tests were tracked under adiabatic conditions when the sample self-heating rate (SHR) exceeded 0.03 °C/min. Experiments were stopped at 350 °C or when the SHR exceeded 20 °C/min. To test the reproducibility of the ARC sample construction and measurements, two identical ARC samples were made and tested for every condition.

### 3. Results and discussion

Fig. 2 shows the SHR versus temperature results on delithiated

Table 2

The chemical composition of the delithiated NMC samples, the molar mass, the full cell capacity and the positive electrode specific capacity for the different NMC grades charged to the different upper cut-off potentials.

Cathode material	Voltage (V)	Chemical formula of delithiated NMC	Molecular mass (g/mol)	Capacity of full cell (mAh)	Specific capacity (mAh/g)
NMC111 (96.4602 g/mol)	4.2	$\text{Li}_{0.424}[\text{Ni}_{1/3}\text{Mn}_{1/3}\text{Co}_{1/3}]\text{O}_2$	92.46	175	160
	4.4	$\text{Li}_{0.363}[\text{Ni}_{1/3}\text{Mn}_{1/3}\text{Co}_{1/3}]\text{O}_2$	92.04	194	177
	4.5	$\text{Li}_{0.327}[\text{Ni}_{1/3}\text{Mn}_{1/3}\text{Co}_{1/3}]\text{O}_2$	91.79	205	187
	4.7	$\text{Li}_{0.18}[\text{Ni}_{1/3}\text{Mn}_{1/3}\text{Co}_{1/3}]\text{O}_2$	90.77	250	228
NMC442 (96.0943 g/mol)	4.2	$\text{Li}_{0.42}[\text{Ni}_{0.42}\text{Mn}_{0.16}\text{Co}_{0.16}]\text{O}_2$	92.07	150	163
	4.4	$\text{Li}_{0.31}[\text{Ni}_{0.42}\text{Mn}_{0.16}\text{Co}_{0.16}]\text{O}_2$	91.3	178	193
	4.5	$\text{Li}_{0.26}[\text{Ni}_{0.42}\text{Mn}_{0.16}\text{Co}_{0.16}]\text{O}_2$	90.96	190	206
	4.7	$\text{Li}_{0.16}[\text{Ni}_{0.42}\text{Mn}_{0.16}\text{Co}_{0.16}]\text{O}_2$	90.26	215	233
NMC532 (96.5545 g/mol)	4.2	$\text{Li}_{0.386}[\text{Ni}_{0.5}\text{Mn}_{0.3}\text{Co}_{0.2}]\text{O}_2$	92.29	180	170
	4.4	$\text{Li}_{0.294}[\text{Ni}_{0.5}\text{Mn}_{0.3}\text{Co}_{0.2}]\text{O}_2$	91.65	207	196
	4.5	$\text{Li}_{0.262}[\text{Ni}_{0.5}\text{Mn}_{0.3}\text{Co}_{0.2}]\text{O}_2$	91.43	217	205
	4.7	$\text{Li}_{0.186}[\text{Ni}_{0.5}\text{Mn}_{0.3}\text{Co}_{0.2}]\text{O}_2$	90.90	239	226
NMC622 (96.93 g/mol)	4.2	$\text{Li}_{0.287}[\text{Ni}_{0.6}\text{Mn}_{0.2}\text{Co}_{0.2}]\text{O}_2$	91.96	170	198
	4.4	$\text{Li}_{0.19}[\text{Ni}_{0.6}\text{Mn}_{0.2}\text{Co}_{0.2}]\text{O}_2$	91.30	192	224
	4.5	$\text{Li}_{0.179}[\text{Ni}_{0.6}\text{Mn}_{0.2}\text{Co}_{0.2}]\text{O}_2$	91.23	195	227
	4.7	$\text{Li}_{0.114}[\text{Ni}_{0.6}\text{Mn}_{0.2}\text{Co}_{0.2}]\text{O}_2$	90.78	210	245
NMC811 (97.2816 g/mol)	4.2	$\text{Li}_{0.022}[\text{Ni}_{0.8}\text{Mn}_{0.1}\text{Co}_{0.1}]\text{O}_2$	91.87	200	215
	4.4	$\text{Li}_{0.15}[\text{Ni}_{0.8}\text{Mn}_{0.1}\text{Co}_{0.1}]\text{O}_2$	91.38	218	234
	4.5	$\text{Li}_{0.13}[\text{Ni}_{0.8}\text{Mn}_{0.1}\text{Co}_{0.1}]\text{O}_2$	91.24	223	239
	4.7	$\text{Li}_{0.06}[\text{Ni}_{0.8}\text{Mn}_{0.1}\text{Co}_{0.1}]\text{O}_2$	90.76	242	260

**Table 3**

Summary of the electrode mass and electrolyte mass used for each ARC test sample.

	4.2 V		4.4 V		4.5 V		4.7 V	
	Electrode (mg)	Electrolyte (mg)	Electrode (mg)	Electrolyte (mg)	Electrode (mg)	Electrolyte (mg)	Electrode (mg)	Electrolyte (mg)
NMC 111	94	30	84	27	80	26	65	21
NMC 442	92	29	77	25	72	23	63	20
NMC 532	88	28	76	24	74	23	65	21
NMC 622	75	24	66	21	65	21	60	19
NMC 811	69	22	63	20	63	20	56	18

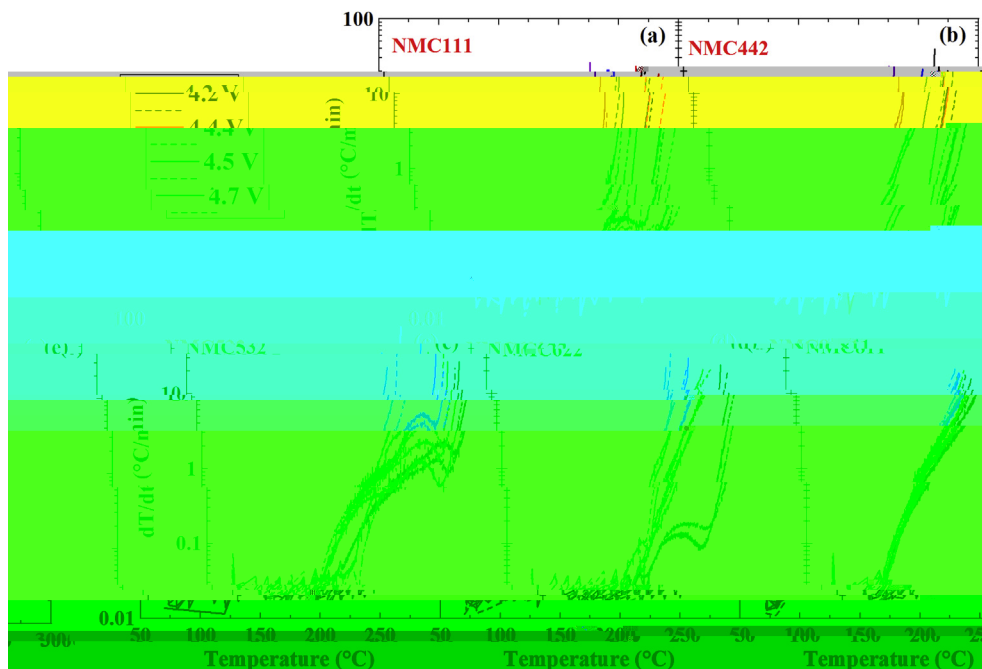


**Fig. 2.** SHR vs. temperature for delithiated (a) NMC111, (b) NMC442, (c) NMC532, (d) NMC622 and (e) NMC811 reacting with control electrolyte at different cut-off voltages. The results for duplicate samples are given as dashed lines in each panel.

(a) NMC111, (b) NMC442, (c) NMC532, (d) NMC622 and (e) NMC811 harvested at various cut-off voltages reacting with control electrolyte. Each experiment was repeated and the results were highly reproducible. The results for duplicate samples are given as dashed lines in each panel. The maximum SHR of all the test samples eventually exceeded 20 °C/min. Fig. 2a shows there is almost no obvious heat release until ~200 °C for NMC111 charged to 4.2 V and that the SHR dramatically increased above ~225 °C. Increasing cut-off potential generally intensified the reaction between charged NMC111 and electrolyte at elevated temperatures. When NMC111 was charged to 4.7 V, the SHR increased dramatically at ~180 °C.

Fig. 2b shows that the SHR NMC442 charged to 4.4 V or 4.5 V is slightly higher than that of NMC442 charged to 4.2 V between ~140 °C and ~190 °C. Then the SHR of NMC442 charged to 4.2, 4.4 or 4.5 V increased significantly at ~225 °C. Like NMC111, the SHR of NMC442 charged to 4.7 V increased dramatically much earlier (~175 °C).

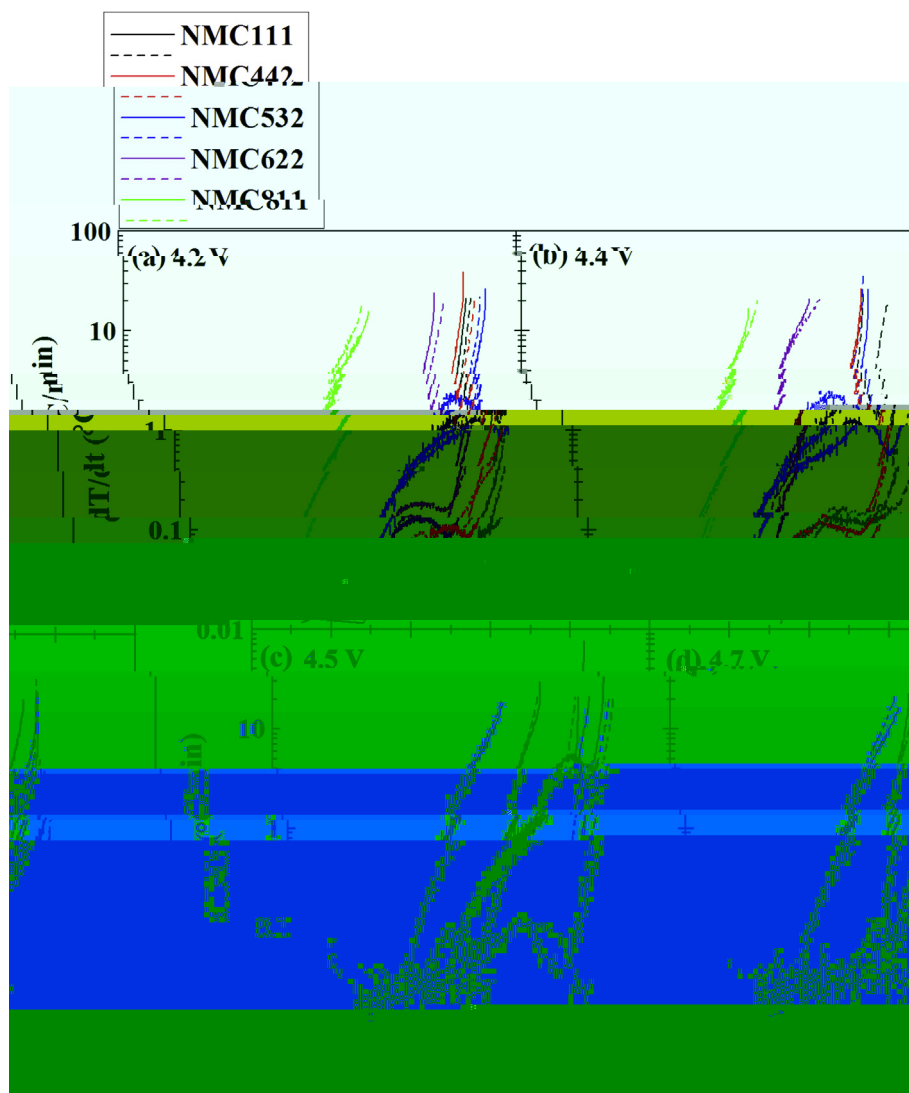
Fig. 2c shows that the onset temperature for a sustained exotherm in NMC532 charged to 4.2, 4.4 or 4.5 V is ~150 °C for all three samples. While reaching the maximum SHR (20 °C/min), the SHRs of NMC532 charged to 4.4 V or 4.5 V are slightly higher than that of NMC532 charged to 4.2 V. The SHR of NMC532 charged to 4.7 V increases dramatically at ~160 °C.

Fig. 2d shows that the onset temperature for a sustained exotherm in NMC622 charged to 4.2, 4.4 or 4.5 V is ~160 °C for all three samples. While reaching the maximum SHR (20 °C/min), the higher the cut-off voltage, the higher the SHR. NMC622 charged to 4.7 V has an earlier onset temperature (~150 °C) and the highest SHR during the exotherm compared to the other cut-off voltages.

Fig. 2e shows that increasing the cut-off voltage does not affect the exothermic behavior of delithiated NMC811. The SHR increases dramatically at 120 °C, which suggests a serious safety concern when NMC811 is used in commercial Li-ion cells.

Fig. 3 shows SHR versus temperature results for the different delithiated NMC grades reacting with control electrolyte at (a) 4.2 V, (b) 4.4 V, (c) 4.5 V and (d) 4.7 V. Fig. 3a–c shows that NMC111 and NMC442 demonstrate similar exothermic behavior over the entire temperature range at 4.2 V, 4.4 V and 4.5 V, respectively. NMC532 and NMC622 are substantially more reactive than NMC111 and NMC 442 at the same potential. NMC811 is dramatically more reactive than the other samples at any potential.

Figs. 2 and 3 compare the various NMC grades at the same potential, but not at the same specific capacity or at the same amount of delithiated Li. In order to make this comparison, the point where the self-heating rate first reached 0.2 °C/min was plotted versus the Li content, x in  $\text{Li}_x[\text{Ni}_x\text{Mn}_y\text{Co}_{1-x-y}]\text{O}_2$ , for each sample (extracted from Table 2). Fig. 4 shows the temperature where the self-heating



**Fig. 3.** SHR vs. temperature results for the different delithiated NMC grades reacting with control electrolyte at (a) 4.2 V, (b) 4.4 V, (c) 4.5 V and (d) 4.7 V. The results for duplicate samples are given as dashed lines in each panel.

rate first reaches  $0.2\text{ }^{\circ}\text{C}/\text{min}$  plotted versus  $x$ . Two results were measured for each data point and the error bar represents the standard deviation between the data. Wang et al. [13] argued that a self-heating rate of  $0.2\text{ }^{\circ}\text{C}/\text{min}$  (in these ARC samples) signifies the temperature where positive electrode-electrolyte reactions will cause thermal runaway in 18650-size cells. Fig. 4 suggests that NMC442 shows excellent safety performance when  $x$  is about 0.25. That is NMC442, at 4.5 V shows less reactivity with electrolyte than NMC111 and NMC532 at 4.4 V and NMC811 at 4.2 V.

#### 4. Conclusions

The reactivity between a series of charged NMC111, NMC442, NMC532, NMC622, NMC811 cathode materials and control electrolyte at elevated temperatures has been systematically investigated using accelerating rate calorimetry. Apart from NMC811, the reactivity of the other NMC materials with electrolyte is affected by the upper cut-off voltage. As the upper cut-off potential increases, the SHR increases, especially at 4.7 V, indicating a trade-off between high energy density and safety. Moreover, the composition of Ni, Mn and Co in NMC-based positive electrode materials also

affects the thermal stability at different cut-off voltages. The amount of  $\text{Mn}^{4+}$  dominates the thermal stability of NMC materials because it is not electrochemically active and can stabilize the oxide matrix even in a highly delithiated state [10,24]. The more Ni in delithiated NMC, the lower the onset temperature of the phase transitions to spinel and rocksalt phases and the larger the amount of released oxygen [25]. The released oxygen will help combust the solvent and produce heat. Therefore, higher Ni content and lower Mn and Co contents generally result in higher SHR and lower onset temperatures for exothermic reactions. Based on the results here, it may be very difficult for NMC811 to be incorporated into safe Li-ion cells with a capacity greater than 1 or 2 A h when traditional EC/EMC electrolyte is used.

Based on the results presented here, NMC442 may offer advantages in terms of cost reduction and safety enhancement compared to the other grades, provided that electrolytes that allow long lifetime to 4.4 or 4.5 V can be found. Other NMC grades such as NMC541 and NMC4.5, 4.5, 1 need to be explored in the future. The information shown in this report will be valuable in guiding battery engineers and researchers to select materials for development or future study that have promise from a safety perspective.

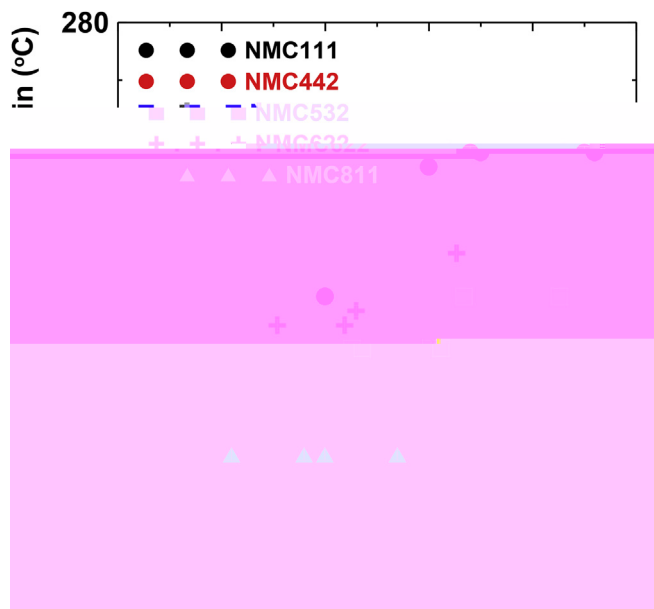


**Fig. 4.** The temperature where the self-heating rate reaches 0.2 °C/min plotted versus the remaining lithium content,  $x$ , in  $\text{Li}_x[\text{NMC}]\text{O}_2$ . This compares all the materials at the same degree of delithiation.

### Acknowledgements

The authors thank NSERC, 3M Canada for the funding of this work under the auspices of the Industrial Research Chairs program. The authors thank Dr. Jing Li of BASF for supplying the  $\text{LiPF}_6$  and the solvents used here.

### References

- [1] B. Scrosati, *Electrochimica Acta* 45 (2000) 2461–2466.
- [2] M.S. Whittingham, *Chem. Rev.* 104 (2004) 4271–4302.
- [3] Y.-K. Sun, C.S. Yoon, S.-T. Myung, I. Belharouak, K. Amine, *J. Electrochem. Soc.* 156 (2009) A1005–A1010.
- [4] A. Yamada, S.C. Chung, K. Hinokuma, *J. Electrochem. Soc.* 148 (2001) A224–A229.
- [5] F. Croce, A.D. Epifanio, J. Hassoun, A. Deptula, T. Olczac, B. Scrosati, *Electrochem. Solid-State Lett.* 5 (2002) A47–A50.
- [6] H. Cao, B. Xia, N. Xu, C. Zhang, *J. Alloy. Compd.* 376 (2004) 282–286.
- [7] K. Kleiner, D. Dixon, P. Jakes, J. Melke, M. Yavuz, C. Roth, K. Nikolowski, V. Liebau, H. Ehrenberg, *J. Power Sources* 273 (2015) 70–82.
- [8] H. Liu, C.R. Fell, K. An, L. Cai, Y.S. Meng, *J. Power Sources* 240 (2013) 772–778.
- [9] H. Yu, H. Zhou, *J. Phys. Chem. Lett.* 4 (2013) 1268–1280.
- [10] H. Kim, S.-M. Oh, B. Scrosati, Y.-K. Sun, *Adv. Battery Technol. Electr. Veh. Woodhead Publ.* (2015) 191–241 accessed 09.12.15.
- [11] Z. Lu, D.D. MacNeil, J.R. Dahn, *Electrochem. Solid-State Lett.* 4 (2001) A200–A203.
- [12] T. Ohzuku, Y. Makimura, *Chem. Lett.* 30 (2001) 642–643.
- [13] Y. Wang, J. Jiang, J.R. Dahn, *Electrochem. Commun.* 9 (2007) 2534–2540.
- [14] H. Kuriyama, H. Saruwatari, H. Satake, A. Shima, F. Uesugi, H. Tanaka, T. Ushirogouchi, *J. Power Sources* 275 (2015) 99–105.
- [15] H. Cao, Y. Zhang, J. Zhang, B. Xia, *Solid State Ion.* 176 (2005) 1207–1211.
- [16] H.-J. Noh, S. Yoon, C.S. Yoon, Y.-K. Sun, *J. Power Sources* 233 (2013) 121–130.
- [17] J. Li, L.E. Downie, L. Ma, W. Qiu, J.R. Dahn, *J. Electrochem. Soc.* 162 (2015) A1401–A1408.
- [18] J. M. Paulsen, L. Y. Kieu, B. G. Ammundsen, US6660432, 2003.
- [19] J. Choi, A. Manthiram, *J. Electrochem. Soc.* 152 (2005) A1714–A1718.
- [20] J. Li, R. Petibon, S. Glazier, N. Sharma, W.K. Pang, V.K. Peterson, J.R. Dahn, *Electrochimica Acta* 180 (2015) 234–240.
- [21] L. Ma, J. Xia, J.R. Dahn, *J. Electrochem. Soc.* 162 (2015) A1170–A1174.
- [22] M. Nie, J. Xia, J.R. Dahn, *J. Electrochem. Soc.* 162 (2015) A1693–A1701.
- [23] D.D. MacNeil, D. Larcher, J.R. Dahn, *J. Electrochem. Soc.* 146 (1999) 3596–3602.
- [24] K.-S. Lee, S.-T. Myung, K. Amine, H. Yashiro, Y.-K. Sun, *J. Electrochem. Soc.* 154 (2007) A971–A977.
- [25] S.-M. Bak, E. Hu, Y. Zhou, X. Yu, S.D. Senanayake, S.-J. Cho, Kwang-Bum Kim, Kyung Yoon Chung, Xiao-qing Yang, Kyung-Wan Nam, *ACS Appl. Mater. Interfaces* 6 (2014) 22594–22601.